# A Robust and Sequential Approach for Detecting Gait Asymmetry Based on Radar Micro-Doppler Signatures

Ann-Kathrin Seifert[‡*], Dominik Reinhard[‡*], Abdelhak M. Zoubir[‡], Moeness G. Amin[†]

[‡] Signal Processing Group
Technische Universität Darmstadt
Merckstr. 25, 64283 Darmstadt, Germany
{seifert, reinhard, zoubir}@spg.tu-darmstadt.de

[†] Center for Advanced Communications
Villanova University
Villanova, PA 19085, USA
moeness.amin@villanova.edu

***Abstract*—Recently, radar has become of increased interest to serve as an unobtrusive sensor for human motion analysis. In particular, for gait analysis, radar could supplement existing technologies to enhance medical diagnostics. Quick turn-around medical evaluation and diagnosis requires reduced data acquisition time which is of interest to patients, doctors, and therapists alike. Hence, we present a robust and sequential approach for detecting gait asymmetry based on radar micro-Doppler signatures. The results obtained based on experimental radar data indicate that high detection rates can be achieved at reduced measurement times compared to conventional approaches.**

***Index Terms*—sequential detection, robustness, gait analysis, Doppler radar, ambient assisted living**

## I. Introduction

Clinical gait analysis plays a central role in diverse applications such as medical diagnosis, rehabilitation and sports. Many neurodegenerative (multiple sclerosis, Alzheimer's, Parkinson's), musculoskeletal (osteoarthritis), or cardiovascular (heart failure) diseases have been shown to alter a person's gait [1]. In particular, many pathological disorders lead to differences between the left and right leg motion, which is referred to as gait asymmetry [2]. Timely detection of gait asymmetry enables early diagnosis and thus can help to ensure proper treatment and improved prognosis.

Recently, a variety of mobile gait analysis systems have been proposed for continuously monitoring a person's gait during activities of daily living (for a review see e.g. [3], [4]). However, since wearable sensors typically need to be worn on the body, they are unfavorable compared to contactless, remote sensing devices, which can observe the gait motions unobtrusively from a distance. In particularly, radar has become of increased interest for human detection and monitoring through walls [5] and in direct line-of-sight [6]. Electromagnetic sensing is safe, privacy-preserving, and insensitive to lighting conditions and clothing. Hence, it may provide an efficient supplement to existing gait analysis systems.

The work of D. Reinhard is supported by the German Research Foundation (DFG) under grant number 390542458. The work of M. G. Amin is supported by the Alexander von Humboldt Foundation, Bonn, Germany.

[*] Both authors contributed equally to this work.

Prior work on using radar for analyzing gait motions has been concerned with person identification [7]–[9], classification of different arm motions [10], [11], and detection of assistive walking devices [12]–[15]. Wang *et al.* [16] utilized pulse-Doppler radar for extracting medically relevant parameters such as the stride rate and walking velocity to characterize a person's gait. In [17], it was recently shown that, based on real radar data, gait asymmetry can be detected with high accuracy for four individuals with different diagnosed gait disorders. However, most of these works assume that, prior to classification, the radar data had already been collected and is available for offline processing. Since the data collection time is often preset, these measurements may take longer than necessary to capture viable motion information. In general, online gait analysis is desirable, where data collection is ceased once we become certain of the underlying motion class.

Rendering quick and reliable decisions is important in many real-time applications [18]. The idea goes back to the 1940s, when Wald developed the sequential probability ratio test (SPRT) [19]. The goal is to perform a hypothesis test with as few samples as possible, while upper-bounding the error probabilities. However, many practical applications suffer from model inaccuracies. Accounting for these inaccuracies calls for robust statistics, which has been an active field of research over the last few decades. An overview of state-of-the-art techniques can be found in, e.g., [20], [21].

In this work, we combine the ideas of robust statistics and sequential analysis to propose an online approach for radar-based gait analysis. To this end, the so-called radar micro-Doppler signatures are analyzed and salient features are extracted, which quantify the (dis)similarity between consecutive steps, and thus, gait (a)symmetry. The distributions of these features under each gait class are obtained by means of kernel density estimation. To account for the inaccuracies of the density estimation, an uncertainty model is used to obtain a set of most similar distributions. These distributions are then employed to construct an SPRT to render a fast and reliable decision about the underlying gait class. Based on real radar data, we show that the proposed approach can achieve high detection rates at reduced measurement durations.

978-9-0827-9703-9/19/$31.00 

The remainder of the paper is organized as follows. Section II details the problem formulation on detecting gait asymmetry sequentially. Section III describes the methodology to solve the given problem. Finally, Section IV presents and discusses experimental results based on real radar data. Section V concludes the paper.

## II. Problem Formulation

Radar back-scatterings of a person's gait contain detailed information on the lower limbs' kinematics. Based on the measured radar signals, we aim at detecting gait asymmetry, which describes the differences between the left and right leg motion. Assuming that a normal gait is symmetrical, and differences between leg motions result in gait asymmetry, we can formulate the problem as a statistical hypothesis test, where

$$\begin{aligned} \mathcal{H}_0: &\quad \text{normal gait}\,, \\ \mathcal{H}_1: &\quad \text{asymmetric gait}\,. \end{aligned}$$

Typically, hypothesis testing is directly performed on the observations. Since modelling the hypothesis test directly in the domain of the observations is intractable, we formulate the problem in the feature domain.

Let $s_n^k$ denote the $k$-th feature, describing the (dis)similarity of two consecutive steps, at time instant $n$, where $k = 1, \ldots, K$ and $n \geq 1$. Assume that the features have a common, time-invariant, distribution $P$, and let $P_0$ and $P_1$ denote the distributions under hypotheses $\mathcal{H}_0$ and $\mathcal{H}_1$, respectively. The two simple hypotheses can then be formulated as

$$\begin{aligned} \mathcal{H}_0: &\quad P = P_0\,, \\ \mathcal{H}_1: &\quad P = P_1\,. \end{aligned} \tag{1}$$

Since the distributions $P_0$ and $P_1$ are neither known nor can be estimated accurately due to the limited amount of training data, the uncertainty caused by the density estimation has to be incorporated in the problem formulation. There exist various ways to model distributional uncertainties like, e.g., the $\varepsilon$-contamination model introduced by Huber [22] or Kassam's band model [23]. The former assumes that a small fraction of the data is contaminated by an arbitrary unknown distribution, whereas the latter assumes that the shape of density function is approximately known, i.e., the true density is restricted to lie in a specified band. By using such uncertainty models, the simple hypothesis testing problem in Eq. (1) is converted to the following composite hypothesis testing problem

$$\begin{aligned} \mathcal{H}_0: &\quad P \in \mathcal{P}_0\,, \\ \mathcal{H}_1: &\quad P \in \mathcal{P}_1\,, \end{aligned} \tag{2}$$

where $\mathcal{P}_0$ and $\mathcal{P}_1$ denote the uncertainty sets under $\mathcal{H}_0$ and $\mathcal{H}_1$, respectively. Hypothesis testing problems of this kind are solved by finding a decision rule $\delta$, which minimizes the *maximum* possible type I and type II errors.

Besides robustness, the time delay until making a decision plays a crucial role in many applications. In our case, we aim to make a decision as quick as possible on the asymmetry of the observed gait, so as to reduce patient inconvenience and limit any possible pain or strain that could be caused by prolonged gait.

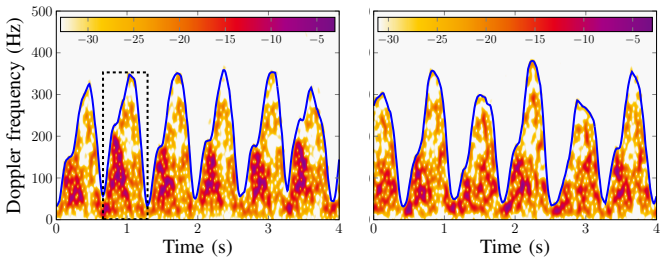


(a) normal (b) asymmetric

Fig. 1: Micro-Doppler signatures of a person walking on a treadmill, where (a) shows normal walking and (b) an asymmetric gait. The colors indicate the energy level in dB.

The need for quick decisions calls for sequential hypothesis testing as introduced by Wald in the late 1940s [19]. Sequential hypothesis tests should minimize the *average* number of used samples while ensuring that the type I and type II errors do not exceed specific bounds set by the designer. Besides a decision rule, a stopping rule has to be found, since the sample size used by a sequential hypothesis test is not known beforehand, and is in fact a random variable.

In essence, based on sequentially observed features of the radar signals, our goal is prompt detection of gait asymmetry using robust sequential hypothesis testing, where type I and type II error probabilities are restricted.

## III. Methodology

### A. Radar Micro-Doppler Signatures of Human Gait

Radar back-scatterings of human motions are typically represented in the time-frequency domain, since the multi-component signals are highly non-stationary. These Doppler frequency vs. time representations reveal the so-called micro-Doppler signatures, which are characteristic to the observed motions [24]. In order to analyze the micro-Doppler signatures in the joint-variable domain, the spectrogram is typically calculated. As an example, Fig. 1 shows two spectrograms of a person walking on a treadmill. The $4\,\mathrm{s}$ measurement of a normal gait in Fig. 1a reveals 6 steps, where the maximal Doppler shift of approximately $350\,\mathrm{Hz}$ is caused by the swinging feet. Fig. 1b shows the same person walking asymmetrically. It is noted that, in this experiment, every second step signature has a lower maximal Doppler frequency. This behavior relates to a confined leg motion, where the observed radial velocity is reduced compared to a normal step.

From the noise-reduced spectrogram, the envelope signal of the micro-Doppler components is calculated using a thresholding technique [14]. In Fig. 1, the envelope signals are represented by a blue line. Next, individual micro-Doppler step signatures are extracted as indicated by the black dashed box in Fig. 1a. Here, the step durations are determined based on local minima in the envelope signal. The individual micro-Doppler

step signatures are considered up to the corresponding maximal observed Doppler shift. Finally, the step signatures are normalized and re-sized to have the same dimensions. These signatures are denoted by $f_n(x,y) \in [0,1]$ for $x = 1,\dots,M_x$ and $y = 1,\dots,M_y$, where $n$ denotes the step count.

### B. Feature Extraction

Since we aim to detect differences between the right and left leg motion, we consider two consecutive step signatures at a time, i.e., $f_{n-1}(x,y)$ and $f_n(x,y)$, and calculate image-based features to quantify the (dis)similarity of the steps. Specifically, for each newly observed step signature $f_n(x,y)$, we compute the $k$-th feature as $s_n^k = g^k(f_{n-1}(x,y), f_n(x,y))$, where $g^k$ describes the $k$-th similarity measure between the step signatures, and $n \geq 1$ represents the step count. We consider a subset of the similarity measures proposed in [17], namely:

- correlation coefficient of full signature,
- correlation coefficient at high Doppler frequencies,
- correlation coefficient at medium Doppler frequencies,
- mean squared error,
- mean absolute deviation.

### C. Robust Sequential Hypothesis Testing

In order to quickly detect gait asymmetry, we resort to Wald's famous SPRT [19]. Each feature is interpreted as a time series and an SPRT is then applied to every feature to decide whether we observe a symmetric or an asymmetric gait. Thus, at each time instant $n$, we observe one realization of the $k$-th feature, $s_n^k$ and compute the likelihood ratios for all $k = 1,\dots,K$, i.e.,

$$\Lambda_n^k = \frac{p_1^k(s_1^k,\dots,s_n^k)}{p_0^k(s_1^k,\dots,s_n^k)} = \prod_{i=1}^{n} \frac{p_1^k(s_i^k)}{p_0^k(s_i^k)}\,. \tag{3}$$

For the sake of compactness, the argument of the densities is dropped and should be clear from the context. We observe new samples from feature $k$ as long as the likelihood ratio $\Lambda_n^k$ stays in some corridor defined by the upper and lower thresholds $A$ and $B$, respectively. Once the lower threshold is crossed, we stop and decide in favor of the null hypothesis, and for the alternative once the upper threshold is crossed. The decision for feature $k$ at time instant $n$ is denoted by $\delta_n^k$. The run-length of the test, i.e., the number of used samples, is hence given by

$$\tau^k : \min\{n \geq 1 : \Lambda_n^k \notin (A,B)\}\,.$$

The thresholds $A$ and $B$ of the sequential test are determined according to Wald [19]

$$A = \frac{1-\beta}{\alpha} \quad \text{and} \quad B = \frac{\beta}{1-\alpha}\,,$$

where $\alpha$ and $\beta$ are the bounds for the type I and type II errors, respectively. Though these thresholds are only asymptotically optimal, i.e., when the bounds of the error probabilities tend to zero, they are easy to compute and sufficient for a wide range of applications.

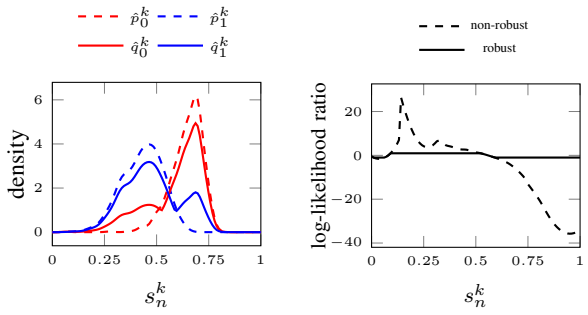


(a) densities (b) log-likelihood ratio

Fig. 2: Example of density functions and the corresponding log-likelihood ratios.

Since the probability density functions $p_0^k$ and $p_1^k$ are not known, they have to be estimated from some training data. For every feature $k = 1,\dots,K$, these densities have to be estimated under both hypotheses, which can, e.g., be done by the use of kernel density estimators. In theory, we can then replace the true densities in the likelihood ratio by their estimates. We remark that due to the limited amount of training data the estimates can become very poor in the tail regions of the densities such that the estimated likelihood ratio breaks down. An example of such behavior is depicted in Fig. 2. One can see that the non-robust log-likelihood ratio takes extremely small/large values in the regions where the densities have their tails. Once an observation falls into one of these regions, the test is forced to stop and make a decision. Since this an unintended behavior of the test, we use Kassam's band model [23] to model deviations from the estimated densities. More precisely, the sets of distributions for both hypotheses are given by

$$\mathcal{P}_i^k = \{p : \underline{p}_i^k \leq p \leq \overline{p}_i^k, \int p(x)\mathrm{d}x = 1\}\,, \tag{4}$$

where $i = 0,1$, and $k = 1,\dots,K$. The band model is a very general uncertainty model, since it includes the $\varepsilon$-contamination model, initially used by Huber [22], as a special case for $\overline{p}_i^k \to \infty$ [25]. The choice of $\underline{p}_i^k$ and $\overline{p}_i^k$ is presented in Section IV-B.

In order to obtain a test which is insensitive to distributional uncertainties, one has to find the pair of distributions of the form in Eq. (4), which minimizes all $f$-divergences, generally referred to as least favorable densities (LFDs). An implicit characterization of the LFDs is given by [25]

$$\begin{aligned} q_0^k &= \min\{\overline{p}_0^k, \max\{c_0(\alpha q_0^k + q_1^k)\}, \underline{p}_0^k\} \\ q_1^k &= \min\{\overline{p}_1^k, \max\{c_1(q_0^k + \alpha q_1^k)\}, \underline{p}_1^k\} \end{aligned} \tag{5}$$

for some $\alpha \geq 0$ and some $c_0, c_1 \in [0, \frac{1}{\alpha}]$. The LFDs are then computed by the iterative algorithm presented in [25].

To obtain a robust SPRT, we replace the densities $p_0^k$ and $p_1^k$ in Eq. (3) by the LFDs $q_0^k$ and $q_1^k$. This results in a log-likelihood ratio which downweights the influence of certain observations, i.e., a single observation cannot force the test to stop directly. An example of the estimated densities and LFDs

is shown in Fig. 2a, and the corresponding log-likelihood ratios are depicted in Fig. 2b.

In summary, our proposed method works as follows: First, the densities $p_i^k$ for $i = 0, 1$, and $k = 1, \ldots, K$ are estimated on a set of training data using a kernel density estimator. Next, we compute a pair of LFDs for each feature. Based on these LFDs, we perform one robust SPRT per feature. Then, the outcomes of the $K$ tests are fused using a majority voting scheme, i.e.,

$$\delta = \arg\max_i \left\{ \sum_{k=1}^{K} \mathbf{1}_{\{\delta^k = i\}} \right\},$$

where $\mathbf{1}_{\{A\}}$ is the indicator function of event $A$. Since we use $K$ different SPRTs in parallel, the number of samples which are required to make a final decision is the one of the slowest SPRT, i.e.,

$$\tau = \max\{\tau^1, \ldots, \tau^K\}.$$

## IV. Experimental Results

### A. Experimental Setup

The experiments were conducted at the Locomotion Laboratory at Technische Universität Darmstadt, Germany (no absorbers). In total, 19 healthy individuals (5 female, 14 male, aged $28.9 \pm 7.5$) were asked to walk on a treadmill for two minutes at two different speeds (0.7 m/s and 1.1 m/s). The experiments were approved by the Technische Universität Darmstadt ethics commission and all volunteers provided written consent. The experimental radar data were collected using a 24 GHz continuous-wave radar [26], which was positioned at approximately knee-height (0.58 m above treadmill surface) and 1.75 m in front of or behind the test subject. In order to enforce asymmetric gait, the angle of deflection of the right knee was confined by an adjustable orthosis. Besides no confinement, which refers to normal, symmetric gait, a confinement angle of 10° was investigated, where the angle describes the extent to which the knee could be bent. Since wearing the orthosis changes the surface of the leg, and thus, its reflection characteristics, a second orthosis was worn on the left leg to ensure comparability between the radar backscatterings from the left and right leg.

For each individual, a set of 16 measurements with a length of 25 s is considered, of which 8 measurements refer to normal walking (no confinement), and the others represent asymmetric gait. Thus, in total, 304 measurements are available, half of which were recorded with a front view (toward) and the other half with a back view (away) on the person. To assess the performance of the proposed method, we apply 10-fold cross validation (10FCV) as well as leave-one-subject-out cross validation (LOSOCV). The former randomly splits the data into 10 folds using stratified sampling with respect to the gait classes to ensure that each fold is representative for the whole dataset. Then, each fold is used for testing once, and the remainder of the data is used for training. The latter performs the splits with respect to the person labels, where data of one subject is kept for testing purposes and the remainder is used for training. As such, this procedure gives an indication on how well the method would perform on a new test subject.

TABLE I: Type I and type II error using the proposed algorithm

| | 10FCV | | LOSOCV | |
|---|---|---|---|---|
| Set | Type I (%) | Type II (%) | Type I (%) | Type II (%) |
| toward | 1.63 | 9.84 | 5.92 | 21.71 |
| away | 3.65 | 3.90 | 7.24 | 10.53 |
| both | 3.12 | 7.08 | 6.91 | 15.79 |

TABLE II: Average measurement duration in units of steps (and seconds).

| | Proposed method | | Entire measurement |
|---|---|---|---|
| Set | 10FCV | LOSOCV | |
| toward | 6.12 (≈ 3.4 s) | 6.19 (≈ 3.4 s) | 45.2 (25.0 s) |
| away | 17.22 (≈ 9.7 s) | 16.16 (≈ 9.1 s) | 44.4 (25.0 s) |
| both | 7.85 (≈ 4.4 s) | 7.50 (≈ 4.2 s) | 44.8 (25.0 s) |

### B. Sequential Detection

Before the results of the proposed algorithm can be presented, the setup has to be described in detail. We estimate the densities under $\mathcal{H}_0$ and $\mathcal{H}_1$ utilizing a kernel density estimator with a Gaussian kernel. The upper and lower bounds used in the band model can, e.g., be set by using confidence intervals. We set the upper bound of the band to infinity and the lower bound to $(1 - \varepsilon)\hat{p}_i^k$, where $\hat{p}_i^k$ is the estimated density of the $k$-th feature under hypothesis $\mathcal{H}_i$. This results in an $\varepsilon$-contamination model with nominal distribution $\hat{p}_i^k$ and contamination rate $\varepsilon$. In the following, the contamination rate is set to 0.2. The upper bounds for the type I and type II errors are set to 10 %. Since we only have pre-recorded data of 25 s per measurement, it can happen that the likelihood ratio of one SPRT is still between the two thresholds $A$ and $B$ once the last sample is reached. In this case, we decide for the hypothesis which is more likely, i.e., we decide for $\mathcal{H}_0$ and $\mathcal{H}_1$ for negative and positive log-likelihood ratios, respectively.

The error probabilities of the proposed algorithm are summarized in Table I. One can see, that for the 10FCV both error probabilities are below the pre-specified 10 % bound. When using LOSOCV, the type I error is below the bound for all datasets. The type II error is only close to the bound for the 'away' scenario, whereas it is far beyond the bound for the other two datasets. In Table II, the average run-length is given. We can see, that on average only a fraction of the respective measurements is used to make a decision.

### C. Comparison to Classifier

Finally, we compare the above results to those of a classifier, that utilizes the entire measurements. Following the approach in [15], we obtain the similarity measures based on averaged micro-Doppler stride signatures, i.e., $s^k = g^k(L(x, y), R(x, y))$, where $L(x, y)$ and $R(x, y)$ denote the average micro-Doppler stride signature of the left and right

TABLE III: Type I and type II error using the NN classifier.

| | 10FCV | | LOSOCV | |
|---|---|---|---|---|
| Set | Type I (%) | Type II (%) | Type I (%) | Type II (%) |
| toward | 2.63 | 2.63 | 3.29 | 3.95 |
| away | 1.97 | 1.97 | 3.29 | 2.63 |
| both | 1.97 | 1.97 | 2.96 | 3.95 |

leg, respectively. Thus, for each measurement, we obtain only one set of features $s^k$, $k = 1, \ldots, K$. Table III shows the results using $K = 5$ features per measurement and a nearest neighbor (NN) classifier. We observe that, given the limited amount of data, the type I error rates are comparable to those obtained by the proposed method. However, the type II errors are considerably smaller for both, 10FCV and LOSOCV, compared to the proposed method. This indicates that the proposed features hold some descriptiveness in the higher dimensions, which are inaccessible by the SPRT.

### D. Discussion

Though the proposed method has large type II errors, while having acceptable type I errors, the average measurement time is reduced by up to a factor of 5. The higher type II errors can be explained as follows. First, only a limited amount of data was available to learn the distributions, which leads to higher type II errors. Second, the NN classifier, which was used for benchmark purposes, directly works in the $K$-dimensional feature space, whereas our proposed method works in the one-dimensional space and performs a majority vote on the $K$ decisions afterwards. Hence, even if the two classes are easily separable in a high-dimensional space, it may be very hard to separate them using the marginal, i.e., one-dimensional, distributions of the features. Future research should be concerned with finding more descriptive features that are possibly even specific for particular gait disorders. Moreover, the proposed method can be extended, such that it uses the entire feature space instead of the marginal distributions of the features.

## V. Conclusion

We presented an approach for online radar-based gait analysis utilizing robust statistics and sequential analysis. Based on real radar-data of 19 individuals, we aimed at detecting gait asymmetry as quickly as possible utilizing streaming-in data. The proposed approach was assessed based on the type I and type II errors, as well as the required average measurement time. Based on the limited data at hand, we showed that high detection rates can by achieved at reduced measurements times. The obtained results were compared to the performance of an NN classifier, which worked with features based on the entire measurements.

## Acknowledgment

The authors would like to thank the Locomotion Laboratory at the Institute of Sport Science, Technische Universität Darmstadt, Germany, for providing the facilities to conduct the experiments. Special thanks to Dr. Martin Grimmer for his support and help with the data collection.

## References

[1] W. Pirker and R. Katzenschlager, "Gait disorders in adults and the elderly," *Wiener Klinische Wochenschrift*, vol. 129, no. 3-4, pp. 81–95, 2017.

[2] A. Gouelle and F. Mégrot, "Interpreting spatiotemporal parameters, symmetry, and variability in clinical gait analysis," in *Handbook of Human Motion*, B. Müller *et al.*, Eds. Springer International Publishing, 2017, pp. 1–20.

[3] A. Muro-de-la Herran *et al.*, "Gait analysis methods: An overview of wearable and non-wearable systems, highlighting clinical applications," *Sensors*, vol. 14, no. 2, pp. 3362–3394, 2014.

[4] S. Chen *et al.*, "Toward pervasive gait analysis with wearable sensors: A systematic review," *IEEE J. Biomed. Health Inform.*, vol. 20, no. 6, pp. 1521–1537, 2016.

[5] C. Debes *et al.*, "Adaptive target detection with application to through-the-wall radar imaging," *IEEE Trans. Signal Process.*, vol. 58, no. 11, pp. 5572–5583, 2010.

[6] Q. Wu *et al.*, "Radar-based fall detection based on doppler timefrequency signatures for assisted living," *IET Radar, Sonar Navigation*, vol. 9, no. 2, pp. 164–172, 2015.

[7] B. Vandersmissen *et al.*, "Indoor person identification using a low-power FMCW radar," *IEEE Trans. Geosci. Remote Sens.*, vol. 56, no. 7, pp. 3941–3952, 2018.

[8] F. K. Teklehaymanot *et al.*, "Bayesian target enumeration and labeling using radar data of human gait," in *26th Eur. Signal Process. Conf. (EUSIPCO)*, 2018.

[9] R. Ricci and A. Balleri, "Recognition of humans based on radar micro-Doppler shape spectrum features," *IET Radar, Sonar & Navigation*, vol. 9, no. 9, pp. 1216–1223, 2015.

[10] F. H. C. Tivive *et al.*, "Classification of micro-Doppler signatures of human motions using log-Gabor filters," *IET Radar, Sonar & Navigation*, vol. 9, no. 9, pp. 1188–1195, 2015.

[11] B. G. Mobasseri and M. G. Amin, "A time-frequency classifier for human gait recognition," in *SPIE Defense, Security, and Sensing*, 2009.

[12] M. S. Seyfioglu *et al.*, "Deep convolutional autoencoder for radar-based classification of similar aided and unaided human activities," *IEEE Trans. Aerosp. Electron. Syst.*, vol. 54, no. 4, pp. 1709–1723, 2018.

[13] S. Z. Gurbuz *et al.*, "Micro-Doppler-based in-home aided and unaided walking recognition with multiple radar and sonar systems," *IET Radar, Sonar & Navigation*, vol. 11, no. 1, pp. 107–115, 2017.

[14] A.-K. Seifert *et al.*, "Radar classification of human gait abnormality based on sum-of-harmonics analysis," in *Proc. 2018 IEEE Radar Conf.*, 2018.

[15] ——, "Toward unobtrusive in-home gait analysis based on radar micro-Doppler signatures," *IEEE Trans. Biomed. Eng.*, 2019, (to be published). [Online]. Available: https://doi.org/10.1109/TBME.2019.2893528

[16] F. Wang *et al.*, "Quantitative gait measurement with pulse-Doppler radar for passive in-home gait assessment," *IEEE Trans. Biomed. Eng.*, vol. 61, no. 9, pp. 2434–2443, 2014.

[17] A.-K. Seifert *et al.*, "Detection of gait asymmetry using indoor Doppler radar," in *IEEE Radar Conf.*, 2019, (to be published). [Online]. Available: http://arxiv.org/abs/1902.09977.

[18] A. Tartakovsky *et al.*, *Sequential analysis: Hypothesis testing and changepoint detection*. Chapman and Hall/CRC, 2014.

[19] A. Wald, *Sequential Analysis*. John Wiley & Sons, 1947.

[20] A. M. Zoubir *et al.*, *Robust Statistics for Signal Processing*. Cambridge University Press, 2018.

[21] ——, "Robust estimation in signal processing: A tutorial-style treatment of fundamental concepts," *IEEE Signal Process. Mag.*, vol. 29, no. 4, pp. 61–80, 2012.

[22] P. J. Huber, "A robust version of the probability ratio test," *Ann. Math. Stat.*, pp. 1753–1758, 1965.

[23] S. Kassam, "Robust hypothesis testing for bounded classes of probability densities (corresp.)," *IEEE Trans. Inf. Theory*, vol. 27, no. 2, pp. 242–247, 1981.

[24] V. C. Chen, *The Micro-Doppler Effect in Radar*. Artech House, 2011.

[25] M. Fauß and A. M. Zoubir, "Old bands, new tracks—revisiting the band model for robust hypothesis testing," *IEEE Trans. Signal Process.*, vol. 64, no. 22, pp. 5875–5886, 2016.

[26] Ancortek Inc., "SDR-KIT 2400AD," http://ancortek.com/sdr-kit-2400ad, retrieved: 09/10/2018.